МИНЕРАЛОГИЧЕСКАЯ КРИСТАЛЛОГРАФИЯ

HYDROGEN BONDING AND STRUCTURAL COMPLEXITY OF CORNETITE, CORNUBITE, ROLLANDITE, AND YVONITE: A THEORETICAL STUDY

© 2020 г. I. V. Kornyakov[1, 2, *] and S. V. Krivovichev[1, 3, **]

[1]*Department of Crystallography, Institute of Earth Sciences, Saint Petersburg State University, University emb., 7/9, Saint-Petersburg, 199034 Russia*

[2]*Laboratory of Nature-Inspired Technologies and Environmental Safety of the Arctic, Kola Science Centre RAS, Fersmana st., 14, Apatity, 184209 Russia*

[3]*Nanomaterials Research Center, Federal Research Center, Kola Science Center RAS, Fersmana st., 14, Apatity, 184209 Russia*

**e-mail: i.kornyakov@spbu.ru*

***e-mail: skrivovi@mail.ru*

Received December 14, 2019; Revised February 11, 2020; Accepted February 12, 2020

Density functional theory has been used to determine positions of hydrogen atoms and to investigate hydrogen-bonding networks in the crystal structures of cornetite, $Cu_3(PO_4)(OH)_3$, cornubite, $Cu_5(AsO_4)_2(OH)_4$, rollandite, $Cu_3(AsO_4)_2 \cdot 4H_2O$, and yvonite, $Cu(AsO_3OH) \cdot 2H_2O$. While hydrogen bonding in cornetite and cornubite are easy to describe, the hydrogen bonding schemes in the crystal structures of rollandite and yvonite are complex and form one-dimensional hydrogen-bonding networks. Informational-based parameters of structural complexity have been calculated for all hydrated copper arsenates and phosphates in order to estimate the complexity of cornetite, cornubite, rollandite, and yvonite compared to other minerals.

Keywords: cornetite, cornubite, rollandite, yvonite, hydrogen bonding, structural complexity

DOI: 10.31857/S0869605520020033

INTRODUCTION

One of the major tasks in modern structural mineralogy is an understanding of the mechanisms governing organization of inorganic matter at the atomic and nano scales. In order to solve this complex and versatile problem, one needs to know the detailed geometrical and topological features of chemical bonding in minerals. Copper oxysalts are well-known for their structural diversity and chemical complexity (Elliot et al., 2014; Mills et al., 2014; Pekov et al., 2014; Vergasova et al., 2014; Rieck et al., 2015; Chukanov et al., 2015; Pekov et al., 2018) and can be considered as model compounds for the investigation of structural principles for minerals of metals with unique electronic configurations. Copper oxysalt minerals tend to appear in a multitude of geochemical environments, including primary ores, oxidation zones of ore deposits, hydrothermal veins and high-temperature dry volcanic fumaroles (Plášil et al., 2014a; 2015b; Pekov et al., 2015a; 2015b). The subject of this study is to model and analyse the hydrogen bonding in cornetite, cornubite, yvonite, and rollandite, four species that belong to the most widespread groups of Cu minerals, arsenates and phosphates.

Cornetite, $Cu_3(PO_4)(OH)_3$, is one of the relatively common copper minerals, which was first described by Cesàro (1912) from the copper mine L'Ètoile du Congo, Katanga, Belgian Congo. Detailed chemical studies of cornetite were reported by Hutchinson and MacGregor (1921), whereas the first diffraction investigation was undertaken by Berry (1950), who deter-

mined its unit-cell parameters and the orthorhombic space group *Pbca*. The crystal structure was solved and refined by Eby and Hawthorne (1989). Cornubite, $Cu_5(AsO_4)_2(OH)_4$, is a triclinic dimorph of cornwallite, which, in turn, is an arsenate analogue of pseudomalachite. The first description of cornubite and its X-ray diffraction pattern were reported by Claringbull et al. (1959). The specimen studied in that work originated from Wheal Carpenter, Gwinear, Cornwall, where it was found in association with quartz and cornwallite. The solution and refinement of the crystal structure of cornubite was reported by Tillmans et al. (1985). The chemical composition and spectroscopic features have been discussed by Janeczek et al. (2016). Rollandite, $Cu_3(AsO_4)_2 \cdot 4H_2O$, was found in the old copper mines of Roua, and described in detail by Sarp and Černý (2000), who provided chemical characterization, X-ray diffraction pattern and crystal structure model for this species. Yvonite, $Cu(AsO_3OH) \cdot 2H_2O$, was reported from the Salsigne mine near Carcassone (Aude, France) (Sarp, Černý, 2000), where it was found in association with chemically and structurally related pushcharovskite, $Cu(AsO_3OH) \cdot 1.5H_2O$, or, more precisely, $K_{0.6}Cu_{18}[AsO_2(OH)_2]_4[AsO_3(OH)]_{10}[AsO_4](OH)_{9.6} \cdot 18.6(H_2O)$ (Pushcharovsky et al., 2000).

As it was described by Costanzo et al. (2007), phosphate minerals may act as phosphate donors to nucleosides, which is important in the understanding of spontaneous phosphorylation process under abiotic conditions. At the same time the paragenesis of phosphate minerals are closely related to the anionic P ↔ As substitutions. For example, published chemical compositions of cornubite (Claringbull et al., 1959; Števko et al., 2011) are very close to the ideal $Cu_5(AsO_4)_2(OH)_4$ stoichiometry as opposite to cornwallite often significantly enriched in P (Števko et al., 2011; Arlt, Armbruster, 1999; Plášil et al., 2009).

The differences in structural architectures have essential influence on the kinetics of phosphorylation reactions, e.g. ludjibaite, pseudomalachite and reichenbachite ($Cu_5(PO_4)_2(OH)_4$ polymorphs) display totally different behavior characterized by minimal reactivity (Costanzo et al., 2007; Huminicki, Hawthorne, 2002). In addition, copper ions can act as catalysts in phosphorylation reactions (Jones, Burt, 1960) and are involved in the nucleoside phosphorylation activity of enzymes as purine nucleoside phosphorylase (Grenha et al., 2005).

The crystal structures are known for all four minerals, except for the positions of the H atoms, which were not reported in the original studies, due to problems associated with crystal imperfection, poor diffraction data, temperature effects, etc. The purpose of this study was to use density functional theory (DFT) to calculate the hydrogen bonding networks in the four minerals and to analyse them from the point of view of their relative structural complexity estimated using information-theoretical procedures suggested in (Krivovichev, 2012; 2013; 2016).

MATERIALS AND METHODS

Density functional theory (DFT) modeling. The CRYSTAL14 software package was employed for the solid-state DFT calculations (Dovesi et al., 2014). The Peintinger–Oliveira–Bredow split-valence triple-ζ (pob-TZVP) basis sets (Peintinger et al., 2013) were used for all atoms along with the hybrid Becke–3–Lee–Yang–Parr (B3LYP) functional, which provides excellent results for copper oxysalt crystals (Ruiz et al., 2006; Ruggiero et al., 2015; Krivovichev et al., 2016). Geometry optimization was initiated with experimental determined crystal-structure models determined previously for cornetite, cornubite, rollandite, and yvonite (Eby, Hawthorne, 1989; Tillmans et al., 1985; Sarp, Černý, 1998; 2000). The approximate positions of the H atoms have been proposed based on general crystal-chemical arguments. During the DFT optimization, all the non-H atom-positions and unit-cell parameters were kept constant, whereas the positions of the H atoms were allowed to relax. The unrestricted-spin calculation was used and the difference between α and β electrons was maintained for the first 10 cycles. The convergence criterion for the energy was set to 10^{-7} au. The crystallographic data for cornetite, cornubite, rollandite, and yvonite are given in Table 1, the optimized coordinates of the

Table 1. Selected crystallographic data for cornetite, cornubite, rollandite, and yvonite
Таблица 1. Кристаллографические данные для корнетита, корнубита, ролландита и ивонита

Parameter	Cornetite	Cornubite	Rollandite	Yvonite
Formulae	$Cu_3(PO_4)(OH)_3$	$Cu_5(AsO_4)_2(OH)_4$	$Cu_3(AsO_4)_2 \cdot 4H_2O$	$Cu(AsO_3OH) \cdot 2H_2O$
Symmetry	Orthorhombic	Triclinic	Orthorhombic	Triclinic
Space Group	*Pbca*	$P\bar{1}$	*Pnma*	$P\bar{1}$
a, Å	10.854	6.121	5.6906	7.632
b, Å	14.053	6.251	17.061	11.168
c, Å	7.086	6.790	9.732	6.020
α, °	90	92.93	90	89.32
β, °	90	111.30	90	86.55
γ, °	90	107.47	90	74.43
V, Å^3	1080.8	227.1	944.9	493.4
Z	8	1	4	4
Reference	1	2	3	4

References: (1) Eby, Hawthore, 1989; (2) Tillmanns et al., 1985; (3) Sarp, Černý, 2000; (4) Sarp, Černý, 1998.

H atoms of all four minerals could be found in Table 2. Tables 3, 4, and 5 provides basic geometrical parameters of strong hydrogen bonds of all four structures.

Structural complexity calculations. An approach based on quantitative evaluation of structural complexity of minerals by Shannon information theory allows to estimate Shannon information content per atom (I_G) and per unit cell ($I_{G,\,\mathrm{total}}$). According to this approach developed by Krivovichev (2012; 2013; 2016), the complexity of a crystal structure can be quantitatively characterized by the amount of Shannon information that it contains measured in bits (binary digits) per atom (bits/atom) and per unit cell (bits/cell), respectively. The concept of Shannon information, also known as a Shannon entropy, used here originates from information theory and its application to various problems in graph theory, chemistry, biology, etc. The amount of Shannon information reflects diversity and relative proportion of individual objects, e.g., the number and relative proportion of different sites in an elementary unit-cell of a crystal structure. The calculation involves the use of the following equations:

$$I_G = -\sum_{i=1}^{k} p_i \log_2 p_i \ \left[\text{bits/atom}\right], \tag{1}$$

$$I_{G,\mathrm{total}} = -v I_G = -v_i \sum_{i=1}^{k} p_i \log_2 p_i \ \left[\text{bits/cell}\right], \tag{2}$$

where k is the number of different crystallographic orbits (independent crystallographic Wyckoff sites) in the structure and p_i is the random-choice probability for an atom from i^{th} crystallographic orbit, that is:

$$p_i = \frac{m_i}{v}, \tag{3}$$

where m_i is a multiplicity of a crystallographic orbit (i.e. the number of atoms of a specific Wyckoff site in the reduced unit-cell), and v is the total number of atoms in the reduced unit-cell.

The information-based structural complexity parameters for cornetite, cornubite, rollandite, and yvonite were calculated using TOPOS software package (Blatov et al., 2014), and are given in Table 6.

Table 2. The optimized coordinates of the H atoms of cornetite, cornubite, rollandite and yvonite
Таблица 2. Оптимизированные координаты атомов H в корнетите, корнубите, ролландите и ивоните

Atom	*x*	*y*	*z*
	Cornetite		
H1	–0.0188	0.3097	0.0065
H2	0.2513	0.1411	0.1544
H3	0.1793	–0.4411	0.3636
	Cornubite		
H1	–0.1993	–0.4287	–0.0508
H2	–0.1936	0.2214	–0.3866
	Rollandite		
H41	0.2594	–0.3516	0.2812
H42	0.3682	–0.3934	–0.3934
H61	0.3518	0.3518	–0.1173
H62	0.0782	0.25	–0.1132
H7	0.2521	0.2045	0.4951
	Yvonite		
H1	0.3604	0.1675	–0.0511
H21	–0.31	0.2122	0.2122
H22	–0.4107	0.3505	0.152
H31	0.2827	0.4207	0.2467
H32	0.3248	0.4697	0.0108
H71	–0.254	0.0209	0.3048
H72	–0.4552	0.0812	0.2365
H81	0.4266	–0.2909	0.3428
H82	0.3437	–0.403	0.2839
H10	0.3984	0.1853	–0.4321

RESULTS

Cornetite. The main features of the crystal structure of cornetite have been described by Fehlmann et al. (1964) and Eby and Hawthorne (1989). There are three symmetrically independent Cu sites. The Cu2 and Cu3 sites are octahedrally coordinated to form strongly distorted CuO_6 octahedra containing four short (1.920–2.022 Å) and two long (2.289–2.820 Å) bonds each. The Cu1 is surrounded by five anions in a distorted square-pyramidal arrangement with four short (1.922–1.995 Å) and one long (2.469 Å) bonds. All the Cu^{2+} coordination geometries are in a good agreement with the Jahn–Teller distortion (Jahn, Teller, 1937; Burns, Hawthorne, 1995; 1996). Each Cu^{2+}-centered polyhedron is coordinated by two $(PO_4)^{3-}$ tetrahedral oxoanions formed around one symmetrically independent P site. The crystal structure of cornetite is composed by corrugated layers of Cu^{2+}-centered polyhedra connected *via* $(PO_4)^{3-}$ tetrahedra forming a three-dimensional framework. The layer is based upon chains of corner-sharing Cu2 octahedra extended along [001] direction (Fig. 1*a*). Each octahedron within the chain shares one common edge and one corner with two adjacent Cu1 square pyramids situated on the opposite sides of the chain. The resulting polyhedral ribbons are connected by sharing common edges between $Cu1O_5$ square pyramids with dimers formed by two Cu3 octahedra sharing a common edge. Phosphate groups are located in between the Cu-based polyhedral layers linking them into a complex copper-phosphate framework shown in Fig. 1*b*.

The crystal structure of cornetite contains three symmetrically independent hydroxyl groups. The OH5 group (Fig. 2*a*) is coordinated by three Cu^{2+} cations and forms relatively strong hydrogen bond to the O4 atom with the H···$\mathbf{A_1}$ bond distance of 1.789 Å (**A** = acceptor).

Table 3. Basic geometrical parameters of hydrogen bonding network in the crystal structures of cornetite and cornubite
Таблица 3. Базовые геометрические параметры водородных связей в структурах корнетита и корнубита

D–H	**D**–H, Å	H···**A**, Å	**D**–H···**A**, °	$\mathbf{A}_1$···H···$\mathbf{A}_2$, °	**D**–H···$\mathbf{A}_1$ + **D**–H···$\mathbf{A}_2$ + $\mathbf{A}_1$···H···$\mathbf{A}_2$	**D**···**A**, Å	**A**
				Cornetite			
O5–H5	0.984	1.789	154.8	97.69	358.79	2.711	O4
		2.461	106.3			2.895	O3
O6–H6	0.996	1.736	161.3	101.54	356.74	2.698	O7
O6–H6		2.583	93.9			2.831	O4
O7–H7	0.98	1.727	155.6	–	–	2.651	O1
				Cornubite			
O1–H1	0.992	1.758	159.37	–	–	2.709	O6
O4–H2	0.979	1.958	153	–	–	2.865	O3

Table 4. Basic geometrical parameters of hydrogen bonds in the structure of rollandite
Таблица 4. Базовые геометрические параметры водородных связей в структуре роллandита

D–H	**D**–H, Å	H–**D**–H, °	H···**A**, Å	**D**–H···**A**, °	$\mathbf{A}_1$···H···$\mathbf{A}_2$, °	**D**–H···$\mathbf{A}_1$ + **D**–H···$\mathbf{A}_2$ + $\mathbf{A}_1$···H···$\mathbf{A}_2$	**D**···**A**, Å	**A**
O4–H41	0.986	103.8	1.787	164.6	83.9	360.1	2.758	O6
O4–H41			2.478	111.6			2.985	O1
O4–H42	1.007		1.567	163.7	110.5	360	2.55	O1
O4–H42			2.59	85.8			2.709	O2
O6–H61	0.976	104.7	2.208	126.4	106.5	359.3	2.896	O1
O6–H62	0.991		1.762	173.6	–	–	2.75	O7
O7–H7 (x2)	0.995	102.6	1.679	164.9	–	–	2.652	O1

Table 5. Basic geometrical parameters of hydrogen bonds in the structure of yvonite
Таблица 5. Базовые геометрические параметры водородных связей в структуре ивонита

D–H	**D**–H, Å	H–**D**–H, °	H···**A**, Å	**D**–H···**A**, °	$\mathbf{A}_1$···H···$\mathbf{A}_2$, °	**D**–H···$\mathbf{A}_1$ + **D**–H···$\mathbf{A}_2$ + $\mathbf{A}_1$···H···$\mathbf{A}_2$	**D**···**A**, Å	**A**
O1–H1	0.984	–	1.779	170.5	–	–	2.754	O10
O2–H21	1.002	107.0	1.733	172.4	98.2	359.5	2.729	O7
O2–H21	1.007		2.528	88.9			2.701	O6
O2–H22	0.994		1.72	175.9	–	–	2.712	O3
O3–H31	0.989	104.3	1.712	174.8	–	–	2.699	O9
O3–H32	0.989		1.706	172.9	–	–	2.691	O11
O7–H71	0.979	107.7	1.775	153.4	–	–	2.686	O12
O7–H72	0.978		1.713	154.4	–	–	2.629	O1
O8–H81	0.979	108.3	1.815	176.6	90.6	358.9	2.792	O10
O8–H81			2.539	91.7			2.748	O5
O8–H82	0.994		1.746	175.8	–	–	2.738	O3
O10–H10	0.979	–	2.219	143.6	–	–	3.063	O7

Table 6. The structural complexity parameters for hydrated copper arsenates and phosphates (in the order of increasing complexity)
Таблица 6. Параметры структурной сложности для водных арсенатов и фосфатов меди

Mineral	Space Group	Formulae	*v*, atoms/cell	I_G, bits/atom	$I_{G,\,total}$, bits/cell	Ref.
Theoparacelsite	*Pmma*	$Cu_3(As_2O_7)(OH)_2$	16	2.500	40.000	1
Gilmarite	*P*1	$Cu_3(AsO_4)(OH)_3$	14	3.807	53.303	2, 3
Cornubite	$P\bar{1}$	$Cu_5(AsO_4)_2(OH)_4$	23	3.567	82.042	4
Ludjibaite	$P\bar{1}$	$Cu_5(PO_4)_2(OH)_4$	23	3.654	84.042	5, 6
Olivenite	$P2_1/n$	$Cu_2(PO_4)(OH)$	36	2.948	106.117	7
Lapeyreite	*C*2/*m*	$Cu_3O(AsO_3OH)_2 \cdot 0.75H_2O$	29	3.755	108.881	8
Libethenite	*Pnnm*	$Cu_2(AsO_4)(OH)$	36	3.170	114.117	9
Babanekite	*C*2/*m*	$Cu_3(AsO_4)_2 \cdot 8H_2O$	37	3.480	128.750	10
Pseudomalachite	$P2_1/c$	$Cu_5(PO_4)_2(OH)_4$	46	3.567	164.084	5, 11
Reichenbachite	$P2_1/a$	$Cu_5(PO_4)_2(OH)_4$	46	3.567	164.084	5, 12
Cornwallite	$P2_1/c$	$Cu_5(AsO_4)_2(OH)_4$	46	3.567	164.084	13
Domerockite	$P\bar{1}$	$Cu_4(AsO_4)(AsO_3OH)(OH)_3 \cdot H_2O$	46	4.567	210.084	14
Clinoclase	$P2_1/c$	$Cu_3(AsO_4)(OH)_3$	56	3.807	213.212	2, 15
Yvonite	$P\bar{1}$	$Cu(AsO_3OH) \cdot 2H_2O$	52	4.700	244.423	16
Euchroite	$P2_12_12_1$	$Cu_2(AsO_4)(OH)(H_2O)$	72	4.170	300.235	17
Rollandite	*Pnma*	$Cu_3(AsO_4)_2 \cdot 4H_2O$	100	3.844	384.386	18
Geminite	$C\bar{1}$	$Cu(AsO_3OH) \cdot H_2O$	80	5.322	425.754	19, 20
Cornetite	*Pbca*	$Cu_3(PO_4)(OH)_3$	112	3.807	426.424	21
Slavkovite	$P\bar{1}$	$Cu_{13}(AsO_4)_6(AsO_3OH)_4 \cdot 23H_2O$	139	6.126	851.533	22

References: (1) Sarp, Černý, 2001; (2) Krivovichev, 2017; (3) Sarp, Černý, 1999; (4) Tillmanns et al., 1985; (5) Krivovichev et al., 2016b; (6) Shoemaker et al., 1981; (7) Chen et al., 2008; (8) Sarp et al., 2010; (9) Cordsen, 1978; (10) Plášil et al., 2017; (11) Shoemaker et al., 1977; (12) Anderson et al., 1977; (13) Arlt et al., 1999; (14) Elliot et al., 2013; (15) Eby, Hawthorne, 1990; (16) Sarp, Černý, 1998; (17) Krivovichev et al., 2016a; (18) Sarp, Černý, 2000; (19) Cooper, Hawthorne, 1995; (20) Prencipe et al., 1996; (21) Eby, Hawthorne, 1989; (22) Sejkora et al., 2010.

The **D**–H···$\mathbf{A_1}$ angle (**D** = donor) is equal to 154.8°. The OH5 site also has one longer OH···O contact to the O3 site with the H···$\mathbf{A}_2$ bond distance of 2.461 Å and **D**–H···$\mathbf{A}_2$ angle of 106.3°, which makes it possible to consider its local configuration as an asymmetric three-center hydrogen bond (Jeffrey, Saenger, 1994). Considering this possibility, it is useful to apply a simple test proposed by Partasarathy (1969), according to which the sum of both **D**–H···**A** (θ_1 and θ_2) angles and and the $\mathbf{A}_1$···H···$\mathbf{A}_2$ (α) angles should be approximately equal to 360°. In the case of the OH5 coordination, the sum of the angles is equal to 358.79°, which indirectly confirms our suggestion. The hydrogen atom is 0.08 Å away from the plane defined by the **D**, $\mathbf{A}_1$ and $\mathbf{A}_2$, which is within 0.2 Å set by Taylor et al. (1984) for asymmetric bifurcated bonds. The shortest hydrogen bond of the OH5 group is between adjacent copper polyhedral layers, whereas the longest is within the same layer.

The OH6 hydroxyl group is coordinated by three Cu^{2+} cations as well (Fig. 2*b*) and forms two hydrogen bonds with the bond distances of 1.736 and 2.583 Å, quite similar to the OH5 group. The two **D**–H···**A** angles are equal to 161.3 and 93.9°, whereas the $\mathbf{A}_1$···H···$\mathbf{A}_2$ angle is equal to 101.54°, which gives the total of 356.74°, in agreement with the Partasarathy test. The hydrogen atom is 0.11 Å away from the $\mathbf{A}_1$–**D**–$\mathbf{A}_2$ plane. As in the case of the OH5 group, the strongest hydrogen bond of the OH6 group serves as a connection between two neighboring

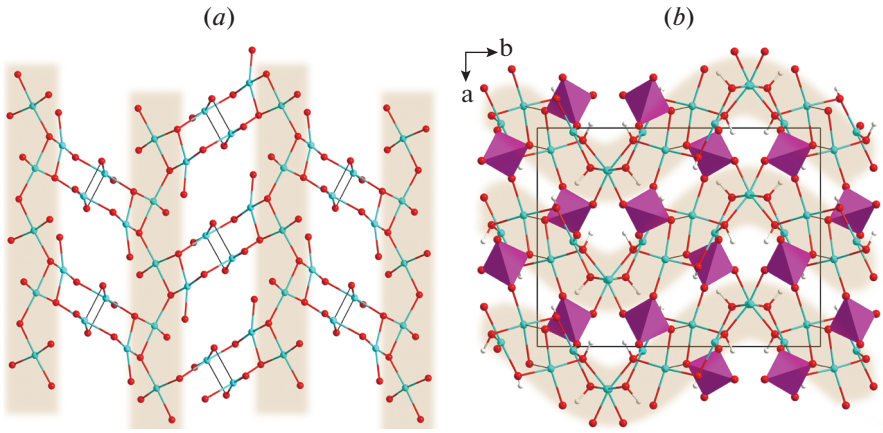

Fig. 1. The layer of Cu^{2+}-centered coordination polyhedra (*a*) and the crystal structure of cornetite (*b*). Legend: Cu atoms = blue, O atoms = red; H = white; PO_4 tetrahedra are shown in pink. The chains of corner-sharing $Cu2O_4$ squares in (*a*) and the Cu-based layers in (*b*) are highlighted in light-brown. The apical bonds of the Cu^{2+}-centered octahedra are removed for clarity.

Рис. 1. Слой Cu^{2+}–центрированных координационных полиэдров (*a*) и кристаллическая структура корнетита (*b*).

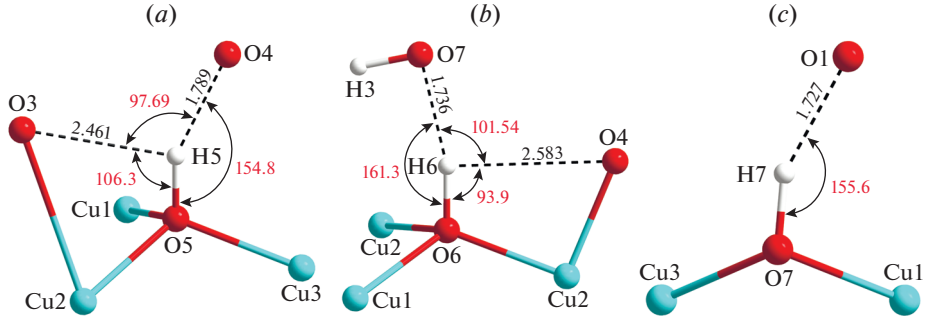

Fig. 2. Local configuration and hydrogen bonding geometry of the OH5 (*a*), OH6 (*b*) and OH7 (*c*) groups in the crystal structure of cornetite.

Рис. 2. Локальная конфигурация и геометрия водородных связей OH5 (*a*), OH6 (*b*) и OH7 (*c*) групп в кристаллической структуре корнетита.

copper-oxygen polyhedral layers. The OH7 group (Fig. 2*c*) forms one two-centered hydrogen bond with the H···**A** bond length of 1.727 Å and the **D**–H···**A** angle of 155.6°. The hydrogen bond is again between two adjacent copper polyhedral layers.

Cornubite. The crystal structure of cornubite contains three symmetrically independent Cu^{2+} cations octahedrally coordinated by O^{2-} anions and $(OH)^-$ groups. All three Cu^{2+}-centered octahedra are elongated with the Cu^{2+}–O_{ap} bond distances varying from 2.320 to 2.468 Å, whereas the Cu^{2+}–O_{eq} bond lengths are in the range of 1.911–2.031 Å. The CuO_6 octahedra are connected by sharing common edges to form infinite brucite-like sheets parallel to $(0\bar{1}1)$

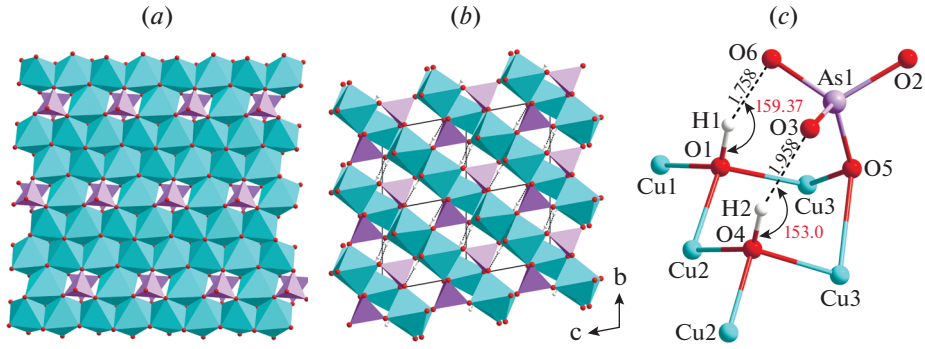

Fig. 3. Brucite like sheet (*a*), crystal structure (*b*) and hydrogen bonds (*c*) in the structure of cornubite.
Рис. 3. Бруситоподобный слой (*a*), кристаллическая структура (*b*) и водородные связи (*c*) в структуре корнубита.

(Fig. 3*a*). Each sheet has vacant octahedral sites capped by $(AsO_4)^{3-}$ tetrahedra above and below the plane of the sheet. The remaining corner of each arsenate group is bonded to three copper cations from the adjacent layer to form a three-dimensional octahedral-tetrahedral framework (Fig. 3*b*).

There are two symmetrically independent hydroxyl groups (Fig. 3*c*) participating in the formation of the Cu^{2+}-centered octahedra. The OH1 group is coordinated by three Cu^{2+} cations and has the **D**–H bond distance of 0.992 Å. The H1 atoms points up towards neighboring octahedral sheet and forms relatively strong two-centered hydrogen bond to the O6 atom belonging to an arsenate group. The H···**A** bond length is 1.758 Å and the **D**–H···**A** angle is equal to 159.37°. The OH4 group has very similar orientation as OH1, but with the shorter **D**–H bond length (0.979 Å) and elongated H···**A** interaction (1.958 Å) and smaller **D**–H···**A** angle (153.0°). The hydrogen bonds are located in the interlayer space and provides additional linkage between adjacent octahedral brucite-like sheets.

Rollandite. There are two symmetrically distinct Cu^{2+} cations in the crystal structure of rollandite. The Cu1 atom is surrounded by six oxygen atoms to form [4 + 2]-distorted CuO_6 octahedra in agreement with the Jahn-Teller effect (Jahn, Teller, 1937; Burns, Hawthorne, 1995; 1996). The Cu2 atom is coordinated by five O^{2-} anions and has a square-pyramidal coordination. The equatorial Cu^{2+}–O_{eq} bond distances vary from 1.933 to 1.999 Å, whereas the Cu^{2+}–O_{ap} lengths are in the range of 2.210–2.583 Å. The shortest apical bond is observed for the square-pyramidal coordination.

The basic structural unit of rollandite is a dioctahedral sheet that can be derived from a brucite-like sheet by removal of certain proportion of cations. The vacant octahedral sites are capped by two $(AsO_4)^{3-}$ tetrahedra, which are attached to the sheet by sharing two corners with Cu^{2+}-centered octahedra (Fig. 4*a*). The third corner of each arsenate tetrahedron coordinates the Cu2 atom in the interlayer space, whereas the fourth acts as an acceptor of hydrogen bonds. The edge-linkage of square pyramids results in the formation of infinite chains located in the interlayer space. The chains alternate with channels filled by H_2O molecules forming a one-dimensional hydrogen-bonding network along the [100] direction (Fig. 4*b*, *c*).

Due to the presence of three symmetrically independent water molecules and diversity of types of hydrogen bonds (two- and three-centered), the hydrogen-bonding network is rather

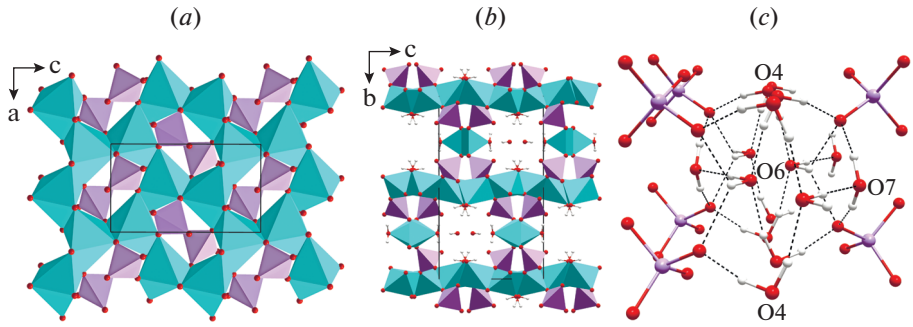

Fig. 4. Octahedral sheet (*a*), crystal structure (*b*) and hydrogen-bonding network (*c*) in rollandite. Legend: Cu polyhedra = blue, As tetrahedra = light-violet, O, As and H atoms are shown as red, violet and white spheres, respectively.
Рис. 4. Октаэдрический слой (*a*), кристаллическая структура (*b*) и сетка водородных связей (*c*) в ролландите.

complicated. The space within the channels is filled by H_2O6 molecules which are stabilized by the connection to the main octahedral-tetrahedral framework *via* hydrogen bonds only. The apical vertices of Cu^{2+}-centered square pyramids and octahedra are occupied by H_2O7 and H_2O4 molecules and oriented towards the channel.

The oxygen atom of the H_2O7 molecule (Fig. 5*a*) is located on the mirror plane and strongly bonded to two symmetrically equal hydrogen atoms. Such an arrangement results in the formation of two symmetrically-related hydrogen interactions, where the **D**–H and H···**A** bond lengths are 0.995 and 1.679 Å, respectively. The O1 atom of $(AsO_4)^{3-}$ group acts as an acceptor for this bond with the **D**–H···**A** angle of 164.9°. Simultaneously, the H_2O7 molecule serves as an acceptor of hydrogen bond formed by the H62 atom belonging to the H_2O6 group. The **D**–H62···**A** angle and H62···**A** bond distances are equal to 173.6° and 1.762 Å, respectively (Fig. 5*b*). The oxygen atom and both symmetrically independent hydrogens of the H_2O6 molecule are located on the mirror plane with the **D**–H bond distances of 0.976 and 0.991 Å. While the H62 atom involved in the two-centered interaction, the H61 atom forms one symmetrical three-centered hydrogen bond with the O1 atom acting as an acceptor. Both H61···**A** interactions are symmetry-related with the H61···**A** bond length equal to 2.208 Å. The **D**–H61···**A** and **A**···H61···**A** angles are equal to 126.4 and 106.5°, respectively. The H_2O6 molecule is an acceptor of the hydrogen bond formed by the H41 atom belonging to the H_2O4 group (Fig. 5*c*). The H41 atom participates in the formation of asymmetric three-centered hydrogen bond with O6 and O1 acting as acceptors. The strongest interaction within this bond is the H41···O6 with the bond distance of 1.787 Å, whereas the H41···O1 bond is essentially longer (2.478 Å). The associated **D**–H41···O6 and **D**–H41···O1 angles are 164.6 and 111.6°, respectively. The $\mathbf{A}_1$···H41···$\mathbf{A}_2$ angle of 83.9° with the sum of all three angles equal to 360.1° satisfies the condition of Partasarathy (1969) and confirms the presence of asymmetric three-centered hydrogen bond. The H41 atom lies within the $\mathbf{A}_1$–**D**–$\mathbf{A}_2$ plane without no significant shift outwards. The H42 atom of the H_2O4 molecule forms a three-centered hydrogen bond as well, with the O1 and O2 atoms serving as acceptors. The H42–O1 and H42–O2 bond distances are equal to 1.567 and 2.590 Å, respectively. Although the H42–O2 bond may seem too elongated to take a part in the formation of an asymmetric three-centered hydrogen bond, the sum of both **D**–H42···**A** and $\mathbf{A}_1$···H42···$\mathbf{A}_2$ angles are equal to 360.0°, and the hydrogen atom lies at 0.01 Å far from $\mathbf{A}_1$–**D**–$\mathbf{A}_2$ plane.

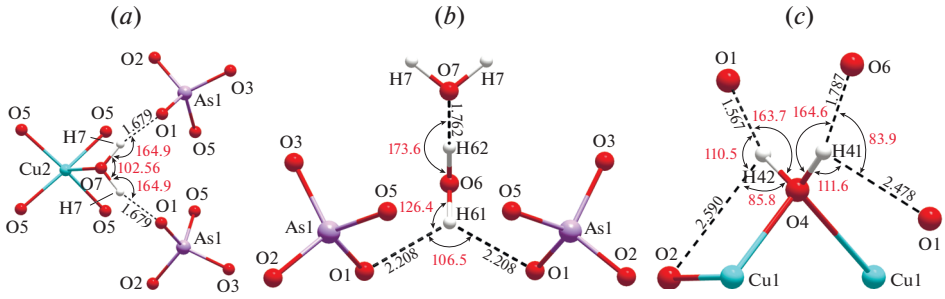

Fig. 5. Hydrogen bonds of H_2O7 (*a*), H_2O6 (*b*) and H_2O4 (*c*) molecules in the structure of rollandite. Legend as in Fig. 4.

Рис. 5. Водородные связи H_2O7 (*a*), H_2O6 (*b*) and H_2O4 (*c*) молекул в структуре ролландита.

The O1 atom of the arsenate group is an acceptor of three strong and one weak hydrogen bonds. Due to the interconnection of all H_2O molecules and the presence of two- and three-centered hydrogen-bonds, a complex infinite hydrogen-bonding network extends along the [100] direction filling the channels within the copper-arsenate framework structure (Fig. 4*c*). This indicates that rollandite may potentially be an one-dimensional proton conductor, but this hypothesis needs an experimental verification.

Yvonite. Two symmetrically distinct Cu^{2+} cations in the crystal structure of yvonite are coordinated by six oxygen atoms each to form typical [4 + 2]-distorted octahedra. The Cu–O_{ap} bond distances vary from 2.558 to 2.828 Å, whereas the Cu–O_{eq} bond distances are in the range of 1.923–1.992 Å. Six corners of each octahedron are occupied by two H_2O molecules and four oxygens belonging to the Asφ_4 (φ = O, OH) tetrahedra to form $CuO_4(H_2O)_2$ octahedra, where H_2O molecules occupy one apical and one equatorial corners in each octahedron. The octahedra share *cis*-edges to form infinite [Cuφ_4] chains extended along [001]. Two chains related by an inversion center are linked along the *b* axis by sharing vertices with the Asφ_4 tetrahedra. The resulting octahedral-tetrahedral sheet (Fig. 6*a*) is parallel to the (100) plane, where (OH) ligands of Asφ_4 tetrahedra remain unconnected to any copper cation and are oriented towards the interlayer space (Fig. 6*b*). Adjacent sheets are connected *via* hydrogen bonds only, formed by (OH) groups of arsenate tetrahedra, H_2O molecules coordinating Cu^{2+} cations, and H_2O molecules located in the interlayer.

There are four symmetrically independent H_2O molecules and two $(OH)^-$ groups. The H_2O2 and H_2O8 molecules coordinate Cu^{2+} cations, whereas the H_2O3 and H_2O7 groups are not directly bonded to any cation. The OH1 group of the As1φ_4 tetrahedron forms, as a donor, one two-centered hydrogen bond with the OH10 group belonging to the As2φ_4 tetrahedron acting as an acceptor (Fig. 7*a*), where both tetrahedra are attached to the same octahedral chain. The **D**–H and H···**A** bond distances are 0.984 and 1.779 Å, respectively, whereas the **D**–H···**A** angle is 170.5°. The OH10 group is involved in relatively weak interaction with the H_2O7 molecule (Fig. 7*b*), which is expressed in the elongated H···**A** and **D**–**A** distances (2.219 and 3.063 Å, respectively) and relatively small **D**–H···**A** angle (143.6°). The OH1 group has also an additional contact to the O12 atom with the H···**A** and **D**–**A** bond lengths of 2.562 and 2.636 Å, respectively. However, the sum of both D–H···**A** and $\mathbf{A}_1$···H···$\mathbf{A}_2$ angles are far from 360°, and thus, it is unlikely that they correspond to any meaningful hydrogen bonds.

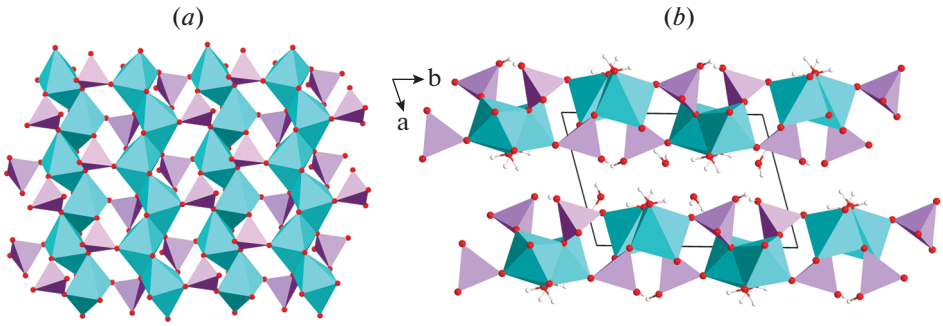

Fig. 6. Octahedral-tetrahedral sheet (*a*) and the crystal structure of yvonite projected along the *c* axis (*b*). Legend as in Fig. 4.

Рис. 6. Октаэдрическо-тетраэдрический слой (*a*) и кристаллическая структура ивонита в проекции на ось *c* (*b*).

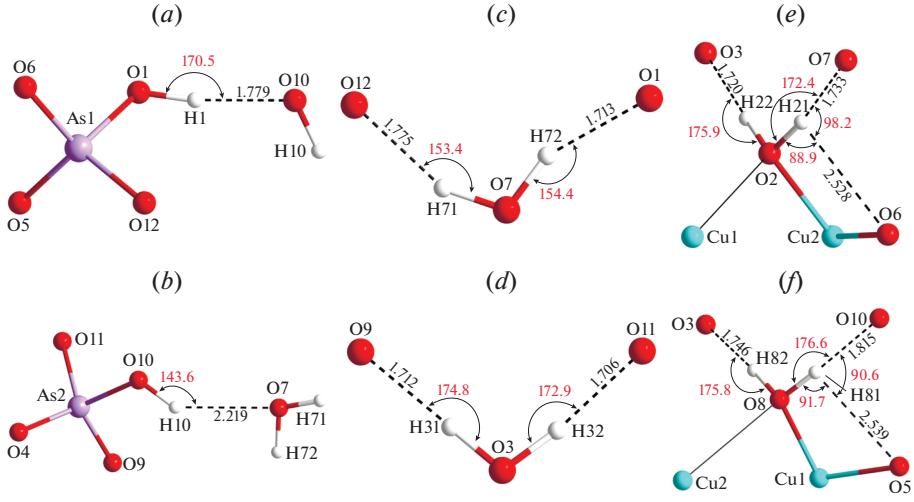

Fig. 7. Hydrogen bonds of OH1 (*a*), OH10 (*b*), H_2O7 (*c*), H_2O3 (*d*), H_2O2 (*e*) and H_2O8 (*f*) molecules in the structure of yvonite.

Рис. 7. Водородные связи OH1 (*a*), OH10 (*b*), H_2O7 (*c*), H_2O3 (*d*), H_2O2 (*e*) и H_2O8 (*f*) молекул в структуре ивонита.

The H_2O7 molecule participates in the connection of two adjacent sheets by forming two hydrogen bonds with the OH1 and O12 atoms (Fig. 7*c*). The **D**–H bond distances are almost the same (0.979 and 0.978 Å, respectively) and the H···**A** distances are similar (1.775 and 1.713 Å, respectively). The **D**–H···**A** angles are similar as well (153.4 and 154.4°, respectively). The H_2O3 molecule, unlike the H_2O7 group, acts as a donor of two two-centered hydrogen bonds to the O9 and O11 atoms (Fig. 7*d*) within the same sheet. The **D**–H bonds are equal (0.989 Å), whereas the H···**A** are very close (1.712 and 1.706 Å) as well as **D**–H···**A** angles (174.8 and 172.9°). Being donors of two hydrogen bonds, the H_2O3 and H_2O7 molecules also act as acceptors of two more hydrogen bonds each.

The H_2O2 group is coordinated by two Cu^{2+} cations and creates one two-centered and one three-centered hydrogen bonds (Fig. 7*e*). The two-centered interaction is between H22 and

H_2O3 with the H···**A** bond length and **D**–H···**A** angle of 1.720 Å and 175.9°, respectively. The H21 atom is involved in asymmetric three-centered interaction, where the closest acceptor is the H_2O7 molecule (1.733 Å) and the distance acceptor is the O6 atom (2.528 Å). The sum of both **D**–H···**A** and $\mathbf{A}_1$···H···$\mathbf{A}_2$ angles are 359.5° and the H21 atom is 0.03 Å far from the $\mathbf{A}_1$–**D**–$\mathbf{A}_2$ plane. A similar bond arrangement is observed for the H_2O8 molecule, which also forms two- and three-centered hydrogen bonds (Fig. 7*f*).

The hydroxyl groups and H_2O molecules form a complex continuous hydrogen-bonding network along *c* axis within the interlayer space. The octahedral-tetrahedral layers are connected directly *via* the H_2O7 molecules as well as indirectly *via* two-step interactions between donors of hydrogen bonds belonging to the layer and H_2O molecules located in the interlayer space.

DISCUSSION

The DFT calculations of positions of the H atoms in the structures under consideration allow us to estimate structural complexity parameters for cornetite, cornubite, rollandite, and yvonite in quantitative terms. The obtained values are listed in Table 6 along with the similar parameters calculated for other natural hydrated copper arsenates and phosphates (we consider only Cu-containing arsenate and phosphate species without admixtures of any other cations and/or anions). As it was mentioned above, cornubite is a triclinic dimorph of cornwallite, which has twice as much atoms in the reduced unit-cell and has the double Shannon information amount per unit cell. Another interesting feature of cornubite is general similarity of its structural complexity with its chemical P-analogue ludjibaite. Despite the fact that cornubite and ludjibaite are not isotypic, both structures contain the same amount of atoms in the reduced unit-cells and their amounts of Shannon information per cell are different by 2 bits only. Yvonite and geminite are based upon sheets of the same type. The (100) sheet in yvonite is similar to the (001) sheet in geminite, but the structure of geminite contains two sheets. This fact and the difference in the hydration state results in the doubling of the Shannon information per unit-cell. Geminite is more complex than yvonite, which is expressed in the amount of Shannon information per atom and per unit cell. Simultaneously, geminite is slightly simpler than cornetite, but the amount of Shannon information per atom is higher.

As it was shown by Krivovichev (2018), structural complexity is a function of topological complexity, symmetry reduction, hydration state, and modularity. The main structural units of cornubite and rollandite can be derived from brucite-like sheets, but the structure of rollandite is more complex. This fact can be explained by the presence in rollandite of additional structural unit (chains of edge-sharing Cu^{2+}-centered square pyramids) and complicated character of hydrogen-bonding network due to the intra channel H_2O molecules. Even though the structure of yvonite is triclinic and contains H_2O molecules within the interlayer space, it is simpler than rollandite. At the same time, the most complex structure is observed for cornetite, despite the absence of water molecules and its orthorhombic symmetry. It should be noted that cornetite has the same stoichiometry as gilmarite and clinoclase (except for the replacement of As by P). Having the same amount of Shannon information per atom, the three minerals differ in the amounts of information and atom per unit cell. The structure of clinoclase has four times as much atoms in the reduced unit cell relative to gilmarite. Cornetite is the most complex among the three minerals (and among all hydrated phosphate copper minerals), having twice as much atoms in the reduced cell and double Shannon information per unit cell than clinoclase. The most complex Cu arsenate/phosphate mineral known so far is slavkovite, $Cu_{13}(AsO_4)_6(AsO_3OH)_4 \cdot 23H_2O$ (Sejkora et al., 2010), due to its complex chemistry and the high hydration state.

As it can be seen, the phosphates and arsenates copper-bearing minerals are closely related. Even though olivenite and libethenite have different crystal structures, they are very close to each other considering their structural complexity parameters. The connection between structural information and configurational entropy of crystals (Krivovichev, 2016) allows us to assume a possible structural transition from olivenite structure type to that of libethenite, which is fully agreed with respective high-temperature investigations (Tarantino et al., 2018).

CONCLUSIONS

Using DFT calculations, positions of H atoms have been determined for cornetite, cornubite, rollandite, and yvonite. Whereas cornetite, cornubite and rollandite have three-dimensional framework structures formed by Cu-polyhedra and As/P-tetrahedra, the crystal structure of yvonite is based upon sheets held together by hydrogen bonds only. The crystal structure of rollandite has a pseudo-layered (or pillared layered) framework structure and contains channels occupied by the one-dimensional hydrogen-bonding system, which has a potential for one-dimensional proton-conducting properties. The information-based structural complexity calculations show that cornubite has a rather simple structure, whereas other three minerals belong to the group of the structures with intermediate complexity.

This research was funded by the Russian Science Foundation (grant No. 19-17-00038).

REFERENCES

Anderson J.B., Shoemaker G.L., Kostiner E., Ruszala F.A. The crystal structure of synthetic $Cu_5(PO_4)_2(OH)_4$, a polymorph of pseudomalachite. *Amer. Miner.* **1977**. Vol. 62. P. 115–121.

Arlt T., Armbruster T. Single-crystal X-ray structure refinement of cornwallite, $Cu_5(AsO_4)_2(OH)_4$: A comparison with its polymorph cornubite and the PO_4-analogue pseudomalachite. *N. Jb. Miner. Abh.* **1999**. Vol. 10. P. 468–480.

Berry L.G. On pseudomalachite and cornetite. *Amer. Miner.* **1950**. Vol. 35. P. 365–385.

Blatov V.A., Shevchenko A.P., Proserpio D.M. Applied topological analysis of crystal structures with the program package ToposPro. *Cryst. Growth Des.* **2014**. Vol. 14. P. 3576–3586.

Burns P.C., Hawthorne F.C. Coordination-geometry structural pathway in Cu^{2+} oxysalt minerals. *Canad. Miner.* **1995**. Vol. 33. P. 889–905.

Burns P.C., Hawthorne F.C. Static and dynamic Jahn-Teller effects in Cu^{2+} oxysalt minerals. *Canad. Miner.* **1996**. Vol. 34. P. 1089–1105.

Cesàro G. Sur un nouveau mineral du Katanga. *Ann. Soc. géol. Belgique.* **1912**. V. 39. P. 241–242.

Chen L., Yang H., Downs R.T. Redetermination of olivenite from an untwinned single-crystal. *Acta Cryst. Sect. E.* **2008**. Vol. 64. P. 60–61.

Chukanov N.V., Aksenov S.M., Rastsvetaeva R.K., Lyssenko K.A., Belakovskiy D.I., Färber G., Möhn G., Van K.V. Antipinite, $KNa_3Cu_2(C_2O_4)_4$, a new mineral species from a guano deposit at Pabellón de Pica, Chile. *Miner. Mag.* **2015**. Vol. 79. P. 1111–1121.

Claringbull G.F., Hey M.H., Davis R.J. Cornubite, a new mineral dimorphous with cornwallite. *Miner. Mag.* **1959**. Vol. 32. P. 1–5.

Cooper M.A., Hawthorne F.C. The crystal structure of geminite, $Cu^{2+}(AsO_3OH)(H_2O)$, a heteropolyhedral sheet structure. *Canad. Miner.* **1995**. Vol. 33. P. 1111–1118.

Cordsen A. A crystal-structure refinement of libethenite. *Canad. Miner.* **1978**. Vol. 16. P. 153–157.

Costanzo G., Saladino R., Crestini C., Ciriello F., Di Mauro E. Nucleoside phosphorylation by phosphate minerals. *J. Biol. Chem.* **2007**. Vol. 282. P. 16729–16735.

Dovesi R., Orlando R., Erba A., Zicovich-Wilson C.M., Civalleri B., Casassa S., Maschio, L., Ferrabone M., De La Pierre M., D'Arco P., Noel Y., Causa M., Rerat M., Kirtman B. CRYSTAL14: a program for ab initio investigation of crystalline solids. *Int. J. Quantum Chem.* **2014**. Vol. 114. P. 1287–1317.

Eby R.K., Hawthorne F.C. Clinoclase and the geometry of [5]-coordinate Cu^{2+} in minerals. *Acta Crystallogr. Sect. C.* **1990**. Vol. 46. P. 2291–2294.

Eby R.K., Hawthorne F.C. Cornetite: Modulated Densely-Packed Cu^{2+} Oxysalt. *Miner. Patrol.* **1989**. Vol. 40. P. 127–136.

Elliot P., Kolitsch U., Willis A.C., Libowitzky E. Description and crystal structure of domerockite, $Cu_4(AsO_4)(AsO_3OH)(OH)_3{\cdot}H_2O$, a new mineral from the Dome Rock Mine, South Australia. *Miner. Mag*. **2013**. Vol. 77. P. 509–522.

Elliott P., Cooper M.A., Pring A. Barlowite, $Cu_4FBr(OH)_6$, a new mineral isostructural with claringbullite: description and crystal structure. *Miner. Mag*. **2014**. Vol. 78. P. 1755–1762.

Fehlmann M., Ghose S., Finney J.J. Direct determination of the crystal structure of cornetite, $Cu_3(PO_4)(OH)_3$, by the Monte Carlo method. *J. Chem. Phys*. **1964**. Vol. 41. P. 1910–1924.

Grenha R., Levdikov V.M., Fogg M.J., Blagova E.V., Brannigan J.A., Wilkinson A.J., Wilson K.S. Structure of purine nucleoside phosphorylase (DeoD) from *Bacillus anthracis*. *Acta Crystallogr., Sect. F: Struct. Biol. Cryst. Commun*. **2005**. Vol. 61. P. 459–462.

Huminicki D.M.C., Hawthorne F.C. The Crystal Chemistry of the Phosphate Minerals. In *Phosphates: Geochemical, Geobiological, and Materials Importance*. Ed. *M.L. Kohn, J. Rakovan, J.M. Hughes*. *Rev. Miner. Geochem*. **2002**. Vol. 48. P. 123–135.

Hutchinson A., MacGregor A.M. On cornetite from Bwana Mkubwa, Northern Rhodesia. *Miner. Mag*. **1921**. Vol. 19. P. 225–232.

Jahn H.A., Teller, E. Stability of polyatomic molecules in degenerate electronic states. I. Orbital degeneracy. *Proc. Roy. Soc., Ser A*. **1937**. Vol. 161. P. 220–236.

Janeczek J., Ciesielczuk J., Dulski M., Krzykawski T. Chemical composition and Raman spectroscopy of cornubite and its relation to cornwallite in Miedzianka, the Sudety Mts., Poland. *N. Jb. Mineral. Abh*. **2016**. Vol. 193. P. 265–274.

Jeffrey G.A., Saenger W. Hydrogen Bonding in Biological Structures. Berlin Heidelberg, Springer-Verlag, **1994**.

Jones R. Burt J.R. The separation and determination of sugar phosphates, with particular reference to extracts of fish tissue. *Analyst*. **1960**. Vol. 85. P. 810–814.

Krivovichev S.V. Hydrogen bonding and structural complexity of the $Cu_3(AsO_4)(OH)_3$ polymorphs (clinoclase, gilmarite): a theoretical study. *J. Geosci*. **2017**. Vol. 62. P. 79–85.

Krivovichev S.V. Ladders of information: what contributes to the structural complexity of inorganic crystals. *Z. Kristallogr*. **2018**. Vol. 233. P. 155–161.

Krivovichev S.V. Structural complexity and configurational entropy of crystals. *Acta Crystallogr. Sect. B*. **2016**. Vol. 72. P. 274–276.

Krivovichev S.V. Structural complexity of minerals: information storage and processing in the mineral world. *Miner. Mag*. **2013**. Vol. 77. P. 275–326.

Krivovichev S.V. Topological complexity of crystal structures: quantitative approach. *Acta Crystallogr. Sect. A*. **2012**. Vol. 68. P. 393–398.

Krivovichev S.V., Zolotarev A.A., Pekov I.V. Hydrogen bonding system in euchroite, $Cu_2(AsO_4)(OH)(H_2O)_3$: low-temperature crystal-structure refinement and solid-state density functional theory modeling. *Miner. Petrol*. **2016**a. Vol. 110. P. 877–883.

Krivovichev S.V., Zolotarev, A.A., Popova, V.I. Hydrogen bonding and structural complexity in the $Cu_5(PO_4)_2(OH)_4$ polymorphs (pseudomalachite, ludjibaite, reichenbachite): combined experimental and theoretical study. *Struct. Chem*. **2016**b. Vol. 27. P. 1715–1723.

Mills S.J., Kampf A.R., Christy A.G., Housley R.M., Thorne B., Chen Y.S., Steele I.M. Favreauite, a new selenite mineral from the El Dragón mine, Bolivia. *Eur. J. Miner*. **2014**. Vol. 26. P. 771–781.

Parthasarathy R. The crystal structure of glycylglycine hydrochloride. *Acta Cryst. Sect. B*. **1969**. Vol. 25. P. 509–518.

Peintinger M.F., Oliveira D.V., Bredow T. Consistent Gaussian basis sets of triple-zeta valence with polarization quality for solid-state calculations. *J. Comput. Chem*. **2013**. Vol. 34. P. 451–459.

Pekov I.V., Siidra O.I., Chukanov N.V., Yapaskurt V.O., Belakovskiy D.I., Murashko M.N., Sidorov E.G. Kaliochalcite, $KCu_2(SO_4)_2[(OH)(H_2O)]$, a new tsumcorite-group mineral from the Tolbachik volcano, Kamchatka, Russia. *Eur. J. Mineral*. **2014.** Vol. 26. P. 597–604.

Pekov I.V., Zubkova N.V., Belakovskiy D.I., Yapaskurt V.O., Vigasina M.F., Sidorov E.G., Pushcharovsky D.Y. New arsenate minerals from the Arsenatnaya fumarole, Tolbachik volcano, Kamchatka, Russia. IV. Shchurovskyite, $K_2CaCu_6O_2(AsO_4)_4$ and dmisokolovite, $K_3Cu_5AlO_2(AsO_4)_4$. *Miner. Mag*. **2015**b. Vol. 79. P. 1737–1753.

Pekov I.V., Zubkova N.V., Yapaskurt V.O., Belakovskiy D.I., Vigasina M.F., Sidorov E.G., Pushcharovsky D.Y. New arsenate minerals from the Arsenatnaya fumarole, Tolbachik volcano, Kamchatka, Russia. III. Popovite, $Cu_5O_2(AsO_4)_2$. *Miner. Mag*. **2015**a. Vol. 79. P. 133–143.

Pekov I.V., Zubkova N.V., Pushcharovsky D.Y. Copper minerals from volcanic exhalations – a unique family of natural compounds: crystal chemical review. *Acta Crystallogr. B.* **2018**. Vol. 74. P. 502–518.

Plášil J., Kasatkin A.V., Škoda R., Škácha P. Klajite, $MnCu_4(AsO_4)_2(AsO_3OH)_2(H_2O)_{10}$, from Jachymov (Czech Republic): the second world occurrence. *Mineral. Mag.* **2014**a. Vol. 78. P. 119–129.

Plášil J., Sejkora J., Čejka J., Škoda R., Goliáš V. Supergene mineralization of the Medvedin uranium deposit, Krkonoše Mountains, Czech Republic. *J. Geosci.* **2009**. Vol. 54. P. 15–56.

Plášil J., Sejkora J., Škoda R., Novák M., Kasatkin A.V., Škácha P., Veselovský F., Fejfarová K., Ondruš P. Hloušekite, $(Ni,Co)Cu_4(AsO_4)_2(AsO_3OH)_2(H_2O)_9$, a new member of the lindackerite supergroup from Jáchymov, Czech Republic. *Miner. Mag.* **2014**b. Vol. 78. P. 1341–1353.

Plášil J., Škácha P., Sejkora J., Škoda R., Novák M., Veselovský F., Hloušek J. Babánekite, $Cu_3(AsO_4)_2{\cdot}8H_2O$, from Jáchymov, Czech Republic – a new member of the vivianite group. *J. Geosci.* **2017**. Vol. 62. P. 261–270.

Prencipe M., Pushcharovsky D.Y., Sarp H., Ferraris G. Comparative crystal chemistry of geminite $Cu[AsO_3OH)]H_2O$ and related minerals. *Moscow Univ. Geol. Bull.* **1996.** Vol. 51. P. 51–58.

Pushcharovsky D.Y., Teat S.J., Zaitsev V.N., Zubkova N.V., Sarp H. Crystal structure of pushcharovskite. *Eur. J. Miner.* **2000**. Vol. 12. P. 95–104.

Rieck B., Pristacz H., Giester G. Colinowensite, $BaCuSi_2O_6$, a new mineral from the Kalahari Manganese field, South Africa and new data on wesselsite, $SrCuSi_4O_{10}$. *Miner. Mag.* **2015**. Vol. 79. P. 1769–1778.

Ruggiero M.T., Erba A., Orlando R., Korter T.M. Origins of contrasting copper coordination geometries in crystalline copper sulfate pentahydrate. *Phys. Chem. Chem. Phys.* **2015**. Vol. 17. P. 31023–31029.

Ruiz E., Llunell M., Cano J., Rabu P., Drillon M., Massobrio C. Theoretical determination of multiple exchange couplings and magnetic susceptibility data in inorganic solids: the prototypical case of $Cu_2(OH)_3NO_3$. *J. Phys. Chem. B.* **2006**. Vol. 110. P. 115–118.

Sarp H., Černý R. Description and crystal structure of Yvonite, $Cu(AsO_3OH) \cdot 2H_2O$. *Amer. Miner.* **1998**. Vol. 83. P. 383–389.

Sarp H., Černý R. Gilmarite, $Cu_3(AsO_4)(OH)_3$, a new mineral: its description and crystal structure. *Eur. J. Miner.* **1999**. Vol. 11. P. 549–555.

Sarp H., Černý R. Rollandite, $Cu_3(AsO_4)_2 \cdot 4H_2O$, a new mineral: its description and crystal structure. *Eur. J. Miner.* **2000**. Vol. 12. P. 1045–1050.

Sarp H., Černý R. Theoparacelsite, $Cu_3(OH)_2As_2O_7$, a new mineral: its description an crystal structure. *Arch. Sci.* **2001**. Vol. 54. P. 7–14.

Sarp H., Černý R., Babalik H., Hatipog?lu M., Mari G. Lapeyreite, $Cu_3O[AsO_3(OH)]_2 \cdot 0.75H_2O$, a new mineral: Its description and crystal structure. *Amer. Miner.* **2010**. Vol. 95. P. 171–176.

Sejkora J., Plášil J., Ondruš P., Veselovský F., Císařová I., Hloušek J. Slavkovite, $Cu_{13}(AsO_4)_6(AsO_3OH)_4 \cdot 23H_2O$, a new mineral species from Horní Slavkov and Jáchymov, Czech Republic: description and crystal-structure determination. *Canad. Miner.* **2010**. Vol. 48. P. 1157–1170.

Shoemaker G.L., Anderson J.B., Kostiner E. Refinement of the crystal structure of pseudomalachite. *Amer. Miner.* **1977**. Vol. 62. P. 1042–1048.

Shoemaker G.L., Anderson J.B., Kostiner E. The crystal structure of a third polymorph of $Cu_5(PO_4)_2(OH)_4$. *Amer. Miner.* **1981**. Vol. 66. P. 169–175.

Števko M., Sejkora J., Bačik P. Mineralogy and origin of supergene mineralization at the Farbište ore occurrence near Poniky, central Slovakia. *J. Geosci.* **2011**. Vol. 56. P. 273–298.

Tarantino S.C., Zema M., Callegari A.M., Boiocchi M., Carpenter M.A. Monoclinic-to-orthorhombic phase transition in $Cu_2(AsO_4)(OH)$ olivenite at high temperature: strain and mode decomposition analysis. *Miner. Mag.* **2018**. Vol. 82. P. 347–365.

Taylor R., Kennard O., Versichel W. Geometry of the NH···O=C hydrogen bond. 2. Three-centered ('bifurcated') and four-centered ('trifurcated') bonds. *J. Am. Chem. Res.* **1984**. Vol. 106. P. 244–248.

Tillmanns E., Hofmeister W., Petitjean K. Cornubite, $Cu_5(AsO_4)_2(OH)_4$, first occurrence of single crystals, mineralogical description an crystal structure. *Bull. Geol. Soc. Finl.* **1985**. Vol. 57. P. 119–127.

Vergasova L.P., Semenova T.F., Krivovichev S.V., Filatov S.K., Zolotarev A.A. Jr., Ananiev V.V. Nicksobolevite, $Cu_7(SeO_3)_2O_2Cl_6$, a new complex copper oxoselenite chloride from Tolbachik fumaroles, Kamchatka peninsula, Russia. *Eur. J. Miner.* **2014**. Vol. 26. P. 439–449.

ВОДОРОДНАЯ СВЯЗЬ И СТРУКТУРНАЯ СЛОЖНОСТЬ КОРНЕТИТА, КОРНУБИТА, РОЛЛАНДИТА И ИВОНИТА: ТЕОРЕТИЧЕСКОЕ ИССЛЕДОВАНИЕ

И. В. Корняков[a, b, *], д. чл. С. В. Кривовичев[a, c, **]

[a] *Кафедра кристаллографии, Институт наук о Земле, Санкт-Петербургский государственный университет, Университетская наб. 7/9, Санкт-Петербург, 199034 Россия*

[b] *Лаборатория природоподобных технологий и техносферной безопасности Арктики, КНЦ РАН, ул. Ферсмана 14, Апатиты, 184209 Россия*

[c] *Центр нанотехнологий, КНЦ РАН, ул. Ферсмана 14, Апатиты, 184209 Россия*

**e-mail: i.kornyakov@spbu.ru*

***e-mail: skrivovi@mail.ru*

На основе теории функционала плотности рассчитаны позиции атомов водорода и исследованы сетки водородных связей в кристаллических структурах корнетита, $Cu_3(PO_4)(OH)_3$, корнубита, $Cu_5(AsO_4)_2(OH)_4$, ролландита, $Cu_3(AsO_4)_2 \cdot 4H_2O$, и ивонита, $Cu(AsO_3OH) \cdot 2H_2O$. Если водородные связи в корнетите и корнубите описываются сравнительно легко, то в ролландите и ивоните это описание усложняется за счет образования одномерных сеток водородных связей. Для всех изученных водных арсенатов и фосфатов меди рассчитаны параметры структурной сложности кристаллических структур.

Ключевые слова: корнетит, корнубит, ролландит, ивонит, водородная связь, структурная сложность